Light Metals 2012 *Edited by: Carlos E. Suarez*
TMS (The Minerals, Metals & Materials Society), 2012

STUDY OF HOMOGENIZATION TREATMENTS OF CAST 5xxx SERIES Al-Mg-Mn ALLOY MODIFIED WITH Zn

Akram Halap, Tamara Radetić, Miljana Popović and Endre Romhanji
Department of Metallurgical Engineering, Faculty of Technology and Metallurgy, University of Belgrade,
Karnegijeva 4, 11000 Belgrade, Serbia

Keywords: Al-Mg alloy, $Al_6(Mn,Fe)$, $Al_{10}Mn$, homogenization

Abstract

Microstructural changes of DC-cast 5xxx series Al-Mg-Mn alloy modified with Zn addition occurring during the homogenization treatments were studied through the thickness of a rolling ingot. The homogenization treatments included: low temperature annealing at 430 °C for 12h and high temperature homogenization at 550 °C for 16h. Microstructure evolution was followed by electrical resistivity measurements, optical microscopy, SEM and TEM characterization and microanalysis. During the homogenization, decomposition of the supersaturated solid solution, present in the as-cast state, occurred. Distribution of the precipitates was dictated by segregations and could be related to the partition coefficients of alloying elements. It was found that during the high temperature homogenization not only dissolution processes occurred, but also precipitation of new phases.

Introduction

Aluminum-magnesium alloys, traditionally used in marine applications, are characterized with a high Mg content that provides high strength. However, Mg presence at levels greater than 3.5 wt.% also makes those alloys susceptible to stress corrosion cracking. Recent research and development [1, 2] in the field have been directed toward increase of a ratio between strength and specific weight of the alloys as well as at increasing a corrosion resistance and strength of a weld. Minor additions of Zn (>0.4 wt.%) to Al-Mg alloys can significantly improve corrosion properties [3, 4]. In addition, these alloys contain other alloying elements such as Mn, Cr, etc. The result of the heavy alloying is that a cast ingot tends to be characterized by the chemical and structural inhomogeneities. Homogenization treatments aim at the elimination of microsegregations as well as achieving favorable distribution and morphology of intermetallic precipitates formed during solidification and subsequent heat treatment. The precipitate distribution, size and morphology are of a particular importance since they have significant effect on a formability and recrystallization of the alloys. There are several published studies on the homogenization treatment of the aluminum alloys from 5xxx series [5-12]. However, understanding of the microstructure evolution during the different stages of homogenization treatment is quite limited. One of the first studies on the homogenization treatments by Sheppard et al [5, 6] described the microstructure evolution of the AA 5083 and AA 5xxx alloys that underwent different homogenization routes, but the study was limited on qualitative descriptions and no phases and precipitates were identified. On the other hand, studies like Lee et al [7, 8] and Ratchev et al [9] were focused on the crystallography of the particular phases present in the alloy and not on the effect of a heat treatment on the microstructure. In this study, we investigated the effects of alloying elements on the microstructure and formation of intermetallic precipitates and eventual changes in the precipitates composition during the homogenization treatment.

Experimental Procedure

Material used in this study was industrially DC cast rolling ingot with dimensions: 1150 mm × 330 mm × 3630 mm. Chemical composition of the alloy is given in Table I.

Table I Chemical composition of the 5xxx alloy (wt.%)

Mg	Mn	Cu	Fe	Si	Zn	Cr	Ti	Sr
5.13	.718	.128	.337	.11	.513	.008	.0254	.003

In order to study effect of the local cooling rate in the ingot on the microstructure, the specimens were cut in transverse direction along the half width line of the ingot (Figure 1).

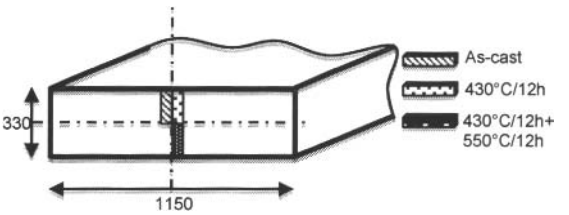

Figure 1. Three blocks were cut from the central part of the ingot along transverse direction and heat treated accordingly. For microstructure characterization and resistivity measurements each block was then cut in eight smaller blocks with dimensions 20 mm × 20 mm × 20 mm.

Three states were characterized: (1) as-cast; (2) annealed at 430 °C for 12 h; (3) annealed at 430 °C for 12h + 550 °C for 16 h. Microstructural characterization was conducted by optical microscopy (OM), scanning electron microscopy (SEM) and transmission electron microscopy (TEM) and microanalysis. Specimens for identification and characterization of distribution of the secondary phases by OM and SEM were prepared by a fine mechanical polishing, while grain size and dendrite arm spacing were determined after electrolytic etching of the specimens using Barker's reagent. Specimens for the TEM characterization were electropolished in a CH_3OH:HNO_3=3:1 solution in the Fishione Twin Jet Polisher. The electropolishing conditions were U=10 V, I=21 mA and T= -35 °C. TEM characterization and microanalysis were conducted in microscopes: JEOL 100CX at 100 kV and

Philips CM200 with EDS detector, at 200 kV. SEM characterization was conducted in a JEOL JSM-6610LV at 20 kV. The electrical resistivity measurements at room temperature were carried on a Sigmatest 2.069 instrument using 60 kHz operating frequency. The size of the specimens used in the measurements was 30 mm × 30 mm × 25 mm.

Experimental Results and Discussion

Electrical properties such as electrical resistivity are very sensitive to the presence of point defects in materials. In alloys, changes in the electrical resistivity reflect changes in a solute content in the alloy matrix, providing an excellent tool to follow precipitation/ dissolution processes in the alloy [13-15]. Variation of the electrical resistivity through thickness of the ingot at different stages of the thermal treatment is shown in Figure 2.

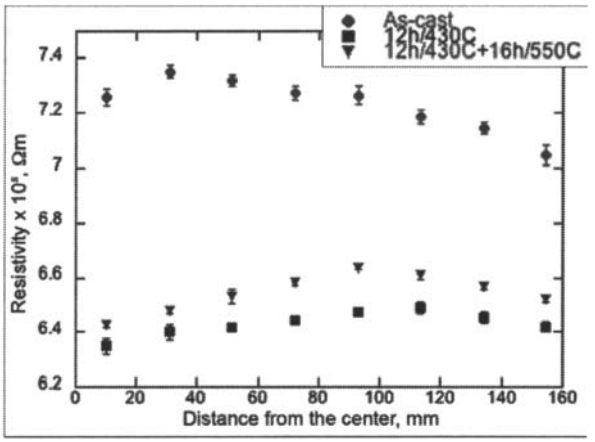

Figure 2. Variation of electrical resistivity throughout the thickness of the ingot after different homogenization stages

In the as-cast state, variation in the electrical resistivity up to 4.2% throughout the ingot thickness indicates presence of segregations. However, there is no abrupt change in the electrical resistivity close to the central part of the ingot to indicate center-line segregations, which is frequently observed in DC cast aluminum sheet ingots [10, 11]. Variation of local cooling rate throughout the ingot thickness affects microstructural characteristics such as grain size, dendrite arms spacing and size of the precipitated eutectic phases. Eutectic precipitates coarsen toward the center of the ingot, but their morphological features do not change significantly (Figure 3). A few morphologically distinct phases were observed by the optical microscopy in the as cast state: block and irregular "Chinese script" phases exhibiting light contrast (A in Figure 3b); a thin, fibrous phase that tends to align along the grain boundaries (B in Figure 3b); strongly faceted phase apparently nucleating on the fibrous phase and is characterized by blue/purple contrast in the optical microscope (C in Figure 3b) and, finally, irregularly shaped dark phase (Figure 4b).

SEM/EDS characterization identified that the phase with block and "Chinese script" morphologies was Al-Fe-Mn based with Mn/Fe ratio favoring Fe (Figure 4a). Selected area electron diffraction patterns during the TEM characterization revealed that the phase had Al_6Mn crystal structure [16]. Coarse, irregularly shaped phase was Al-Mg based, most likely Al_3Mg_2 (Figure 4b).

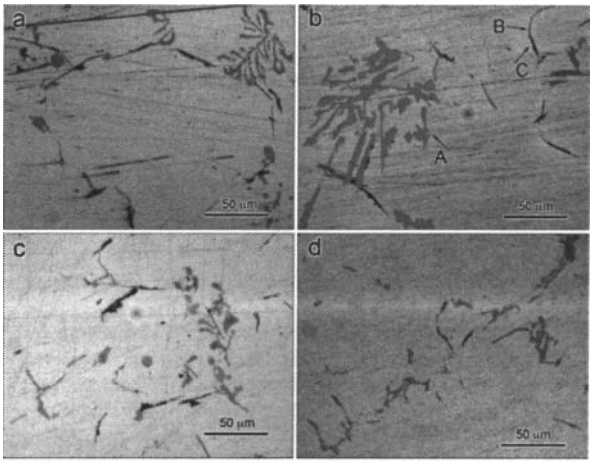

Figure 3. Optical micrographs of the eutectic phases: (a) 10 mm from the ingot center; (b) 51 mm from the ingot center; (c) 101 mm from the ingot center; (d) 150 mm from the ingot center.

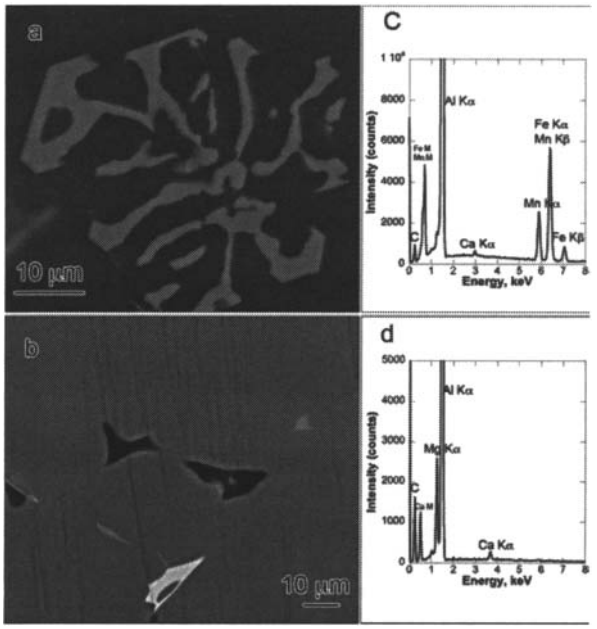

Figure 4. (a) Backscattered electron image of the Fe and Mn rich phase and corresponding EDS spectra; (b) Backscattered electron image of the phase with a dark contrast and irregular shape and corresponding EDS spectra.

More interesting were fibrous and strongly faceted phases (Figure 5). In back scattered electron (BE) images, the fibrous phase had light contrast, while the faceted phase dark. Difference in the contrast can be related to chemical composition of the phases as EDS results showed. Both of phases contained Mg and Si, but

fibrous phase had also Zn and Sr in its composition (Figures 5c and d). Zn and Sr are heavier elements that give rise to lighter contrast in BE images. Observed oxygen peaks on EDS spectra are likely to be result of surface oxidation. Characterization throughout the thickness of the ingot showed that the Zn was mostly concentrated in the fibrous eutectic phase and in the interdendritic regions, due to the very low partition coefficient in Al [17]. Subsequent homogenization treatment did not result in Zn redistribution, as Zn has very low diffusivity in Al [17]. The source of Sr in the alloy was added scrap material, a common practice in the industry. Although Sr content was low, as a strong modifier it had a very strong influence on the morphology of the eutectic phases.

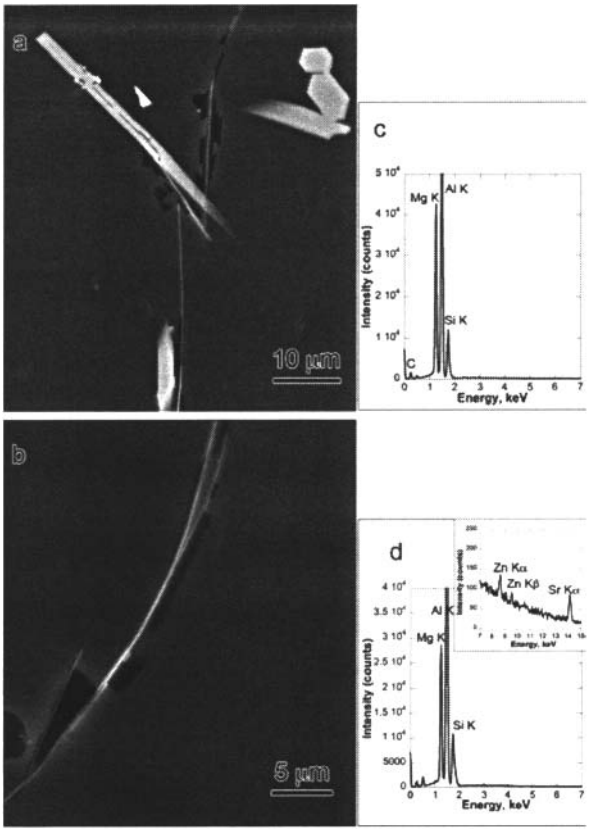

Figure 5. (a) Backscattered electron image of the eutectic phases in the as-cast state. (b) Backscattered electron image of the eutectic phases after annealing for 12h at 430 °C. In both cases it is evident presence of two phases: thin fibrous phase exhibiting light contrast and dark, faceted phase; (c) EDS spectra of faceted phase; (d) EDS spectra of the fibrous phase showing presence of Zn and Sr.

Electrical resistivity of the as-cast state was greater than after subsequent homogenization treatment throughout the ingot thickness (Figure 2), pointing out that the significant part of alloying elements retained in the solid solution during the DC casting. Microstructural characterization showed presence of coarse eutectic phases in the microstructure of the as-cast state (Figures 3 and 4), but TEM investigation on the finer scale did not reveal presence of any dispersioids within grains, but only high dislocation density (Figure 6a). Lack of dispersoids in dendrite cores indicates nucleation barrier or insufficient driving force, as an ingot stays sufficiently long at elevated temperatures in the DC casting, to allow for short-range diffusion and precipitation to occur during cooling.

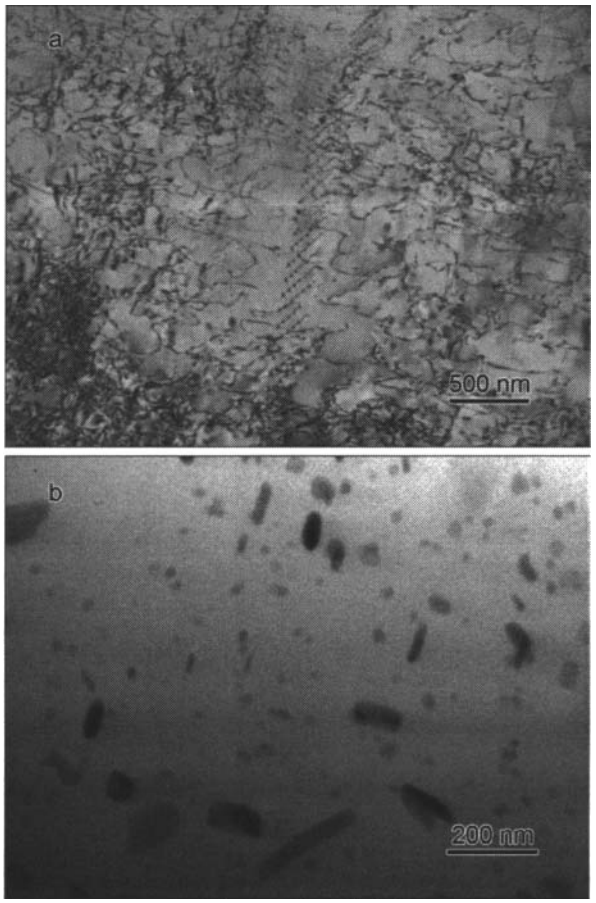

Figure 6. (a) Bright Field TEM micrograph of the microstructure in the as-cast state. High dislocation density was observed, but there is no fine dispersoids. (b) Bright Field TEM micrograph of the microstructure after annealing for 12 h at 430 °C. Fine dispersoids precipitated from the supersaturated solid solution.

Precipitation of fine dispersoids did occur after annealing at 430 °C (Figure 6b). Dispersoid distribution was very homogeneous throughout the specimen, while their morphology ranged from equiaxed to rod shaped. EDS characterization showed that the majority of the precipitates were Al-Mn based, while small fraction contained also Mg. Homogeneous distribution of the dispersion could be related to their chemistry: Mn has partition coefficient close to 1 in Al alloys, hence it does have significant tendency toward segregations [17]. On the other hand, although Mg tends to segregate into interdendritic regions during the solidification, as fast diffuser it has ability to penetrate into dendrite during homogenization treatment.

Annealing at 430 °C did not significantly alter morphology and phase composition of the coarse eutectic particles. Faceted Mg-Si based phase appeared more continuous (Figure 5b). Its nucleation on the $Al_6(Fe,Mn)$ particles was also observed (Figure 7).

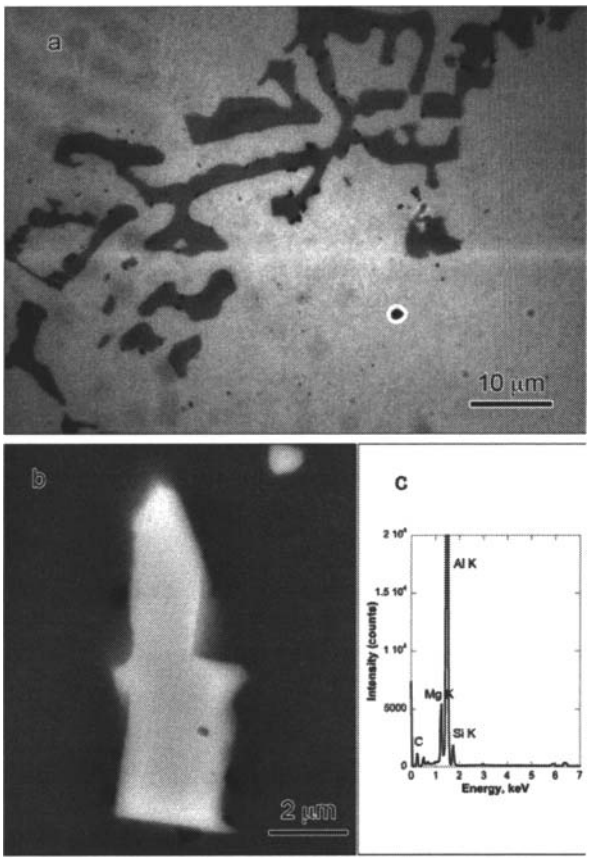

Figure 7. Annealing for 12h at 430 °C resulted in precipitation of Mg-Si based phase on eutectic $Al_6(Fe,Mn)$ particle: (a) Optical micrograph; (b) Backscattered electron image; (c) Corresponding EDS spectra.

After the homogenization at 550 °C for 16h Mg-Si precipitates formed at $Al_6(Fe,Mn)$ particles were dissolved. In addition, partial dissolution and rounding of the facets of $Al_6(Fe,Mn)$ phase was observed (Figure 8) as well as appearance of new dispersoids: rod and plate like particles homogeneously scattered throughout the grains (Figure 8). EDS characterization showed that the precipitated particles were Al-Mn-Fe based, but the Mn/Fe ratio was in favor of Mn (Figure 8c).

TEM characterization revealed that there were two morphologies of these precipitates. Precipitates in the shape of thin plates had $Al_6(Mn)$ crystal structure [16] as shown by indexing their diffractions patterns (Figure 9). Rod-shaped precipitates were coherent/semicoherent with the matrix along the longer axis (Figure 10) and were identified to have crystal structure of hexagonal, metastable $Al_{10}Mn_3$ [16] phase.

It appears that dissolution of $Al_6(Fe,Mn)$ and precipitation of $Al_6(Mn,Fe)$ and $Al_{10}(Mn,Fe)_3$ were synergetic processes. Al_6Fe and Al_6Mn phases are isomorphic compounds with high respective solubility of Mn and Fe [18]. However, while the Mn-based compound is a stable phase, the Fe-based one is metastable [10, 18]. Despite the fact that in the studied alloy manganese content exceeded iron, iron rich eutectic $Al_6(Fe, Mn)$ intermetallic phase was formed during the solidification of the alloy due to the very low partition coefficient of Fe [17] and hence, concentration build up at the liquid/solid interface. During the high temperature homogenization, as metastable eutectic $Al_6(Fe,Mn)$ particles dissolve, but in the same time due to the excess Mn in the solid solution Mn rich dispersoids precipitate.

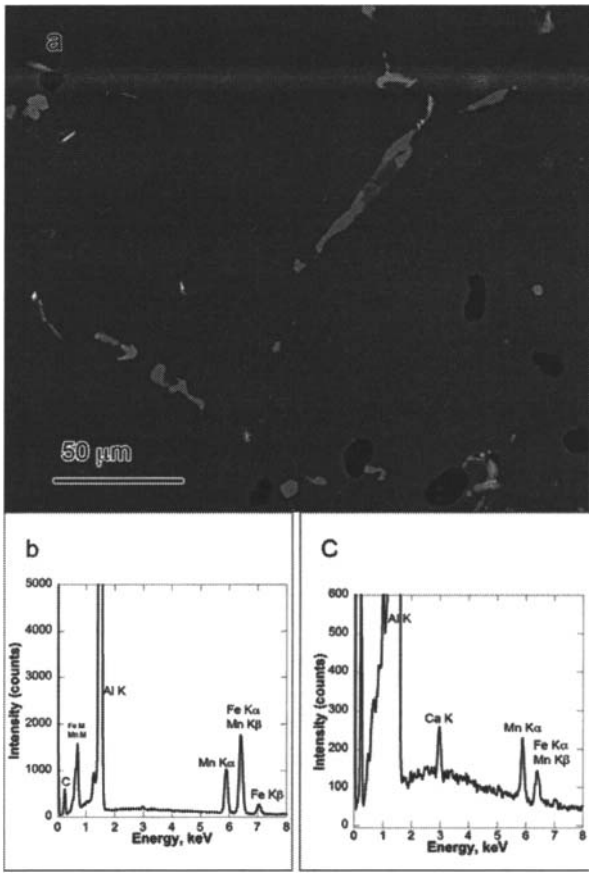

Figure 8. (a) Backscattered electron image of the specimen annealed for 16 h at 550 °C. Rounding and partial dissolution of $Al_6(Fe,Mn)$ eutectoid phase was occurred and uniform precipitation of the rod/plate like Al-Mn-Fe precipitates. (b) EDS spectra of the eutectic phase; (c) EDS spectra of the precipitate.

Conclusion

The study of the effect of homogenization treatment on the microstructure evolution of the industrially cast 5xxx series Al-Mg alloy showed that during the low temperature anneal decomposition of the supersaturated solid solution and precipitation of fine Al-Mn based dispersoids occurred. High temperature anneal at 550 °C resulted not only in partial dissolution of eutectic, metastable iron-based $Al_6(Fe,Mn)$

particles, but also precipitation of plate and rod shaped particles that were Al-Mn-Fe based with Mn/Fe ratio favoring manganese. Electron diffraction patterns revealed that the plate like particles had Al_6Mn crystal structure while rod shaped particles were hexagonal $Al_{10}Mn_3$. Zn was found to segregate into interdendritic regions and it was bound into the eutectic phase with fibrous morphology. Sr, although present in alloy at ppm levels, was found to have large effect on the morphology of eutectic constituents.

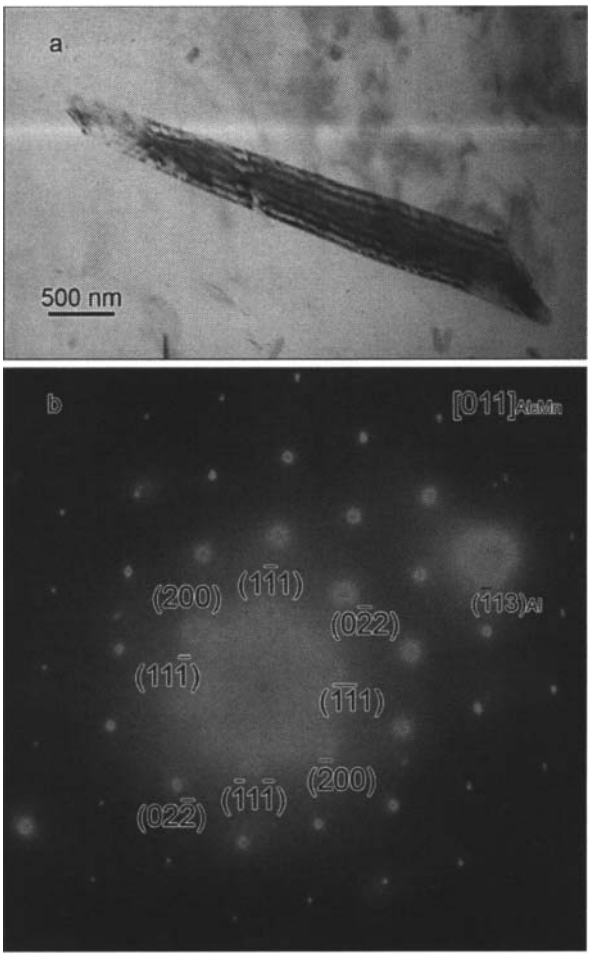

Figure 9. TEM micrographs of the plate-like precipitate (a) Bright field image; (b) Indexed selected area diffraction pattern showing reflections characteristic for Al_6Mn phase [16].

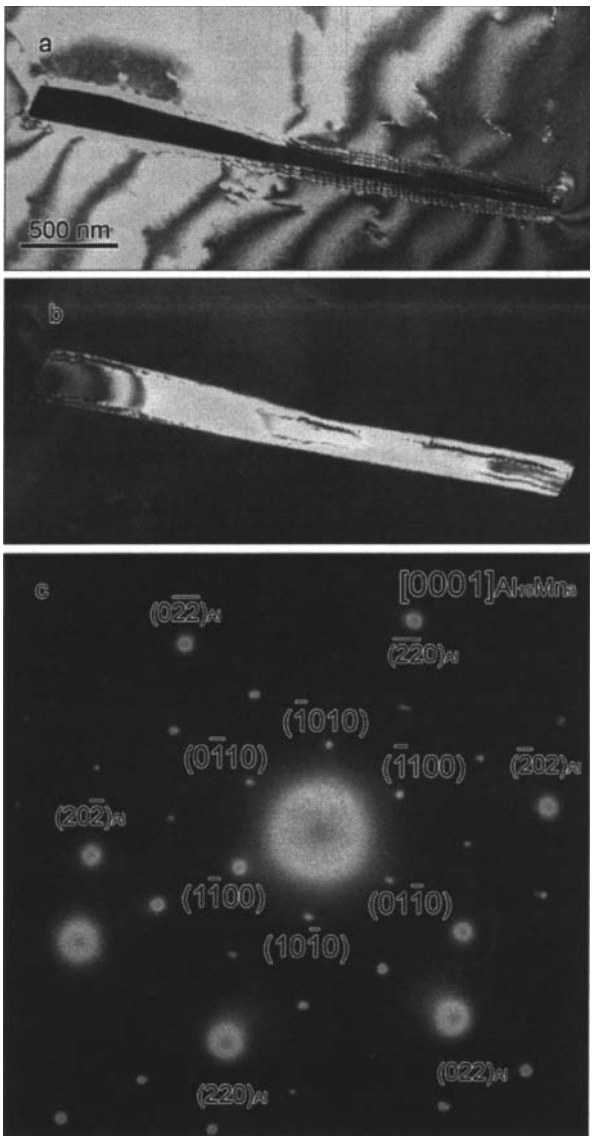

Figure 10. TEM micrographs of the rod-like precipitate (a) Bright field image; (b) Dark field image; (c) Indexed selected area diffraction pattern showing reflections characteristic for $Al_{10}Mn_3$ phase [16].

Acknowledgements

This research was supported by the Ministry of Education and Science, Republic of Serbia, and Impol-Seval Aluminum Mill, Sevojno, under contract number TR 34018 and E!4569.

References

1. G.M. Raynaud, Ph. Gomiero. "The Potential of 5383 Alloy in Marine Applications", In: Proceedings of Alumitech '97 - Transportation, Sponsored by Aluminum Association, Inc., May 20-23, Atlanta; 1997, 353-366.
2. A. Duran, R. Dif. "New Alloy Development at Pechiney: a New Generation of 5383," *Conf. Proc. FAST 2001*, ed. P.A. Wilson and G.E. Hearn, Vol.3, (Southampton: Southampton University; 2001), 223-230.
3. M. C. Carroll et al. "Effects of Zn additions on the grain boundary precipitation and corrosion of Al-5083," *Scripta Mater*, 42 (2000), 335-340.
4. M. C. Caroll et al. US Patent Appl. Pub. No. US 2004/0091386 A1 (May 13, 2004).
5. M.A. Zaidi and T. Sheppard, "Effect of high-temperature soak and cooling rate on recrystallization behavior of two Al-Mg alloys (AA 5252 and AA 5454)" *Met Technol*, 11 (1984), 313-319.
6. T. Sheppard and N. Raghunathan. "Modification of cast structures in Al-Mg alloys by thermal treatments," *Mater Sci Tech*, 5 (1989), 268-280.
7. S.L. Lee and S.T. Wu. "Influence of soaking treatments on hot ductility of Al-4.85 pct Mg alloys containing Mn," *Metall Trans*, 17A (1986), 833-841.
8. S.L. Lee and S.T. Wu. "Identification of dispersoids in Al-Mg alloys containing Mn," *Metall Trans*, 18A (1987), 1353-1357.
9. P. Ratchev, B. Verlinden and P. Van Houtte. "Effect of preheat temperature on the orientation relationship on (Mn,Fe)Al_6 precipitates in an AA 5182 Aluminum – Magnesium alloy," *Acta Metall Mater*, 43 (1995), 621-629.
10. Y.J. Li and L. Arnberg. "Solidification structures and phase selection of iron-bearing eutectic particles in a DC-cast AA5182 alloy," *Acta Mater*, 52 (2004), 2673-2681.
11. Y.J. Li and L. Arnberg. "A eutectoid phase transformation for the primary intermetallic particle from Al_m(Fe,Mn) to Al_3(Fe,Mn) in AA5182 alloy," *Acta Mater*, 52 (2004), 2945-2952.
12. L. Z. He et al. "Effects of homogenization microstructures and properties of a new type Al-Mg-Mn-Zr-Ti-Er alloy," *Mater Sci Eng*, 527A (2010), 7510-7518.
13. J. E. Hatch. *Aluminum: Properties and physical metallurgy* (2nd ed. Metals park Ohio: ASM) 1984.
14. E. Romhanji, M. Popović and S. Stanojević. "Precipitation processes in Al-Mg-(Mn,Cu) type alloy sheets evaluated through electrical resistivity variations," *J Nondestruct Eval*, 29 (2010), 43-48.
15. M. Popović and E. Romhanji. "Characterization of microstructural changes in an Al-6.8wt% Mg alloy sheets by electrical resistivity measurements," *Mater Sci Eng*, A492 (2008), 460-467.
16. P. Villars *Pearson's handbook: Desk edition: Crystallographic data for intermetallic phases* (Rev. Sub Ed., ASM International, 1998), 912-913..
17. M. Easton, C. Davidson and D. St John. "Effect of alloy composition on the dendrite arm spacing of multicomponent aluminum alloys," *Metal Mater Trans*, 41A (2010), 1528-1538.
18. C.A. Ahravci and Ö Pekgüleryüz. "Calculation of phase diagrams for the metastable Al-Fe phases forming in direct-chill (DC)-cast aluminum alloy ingots," *Calphad*, 22 (1998), 147-155.